in Science and Racket Sport Ⅲ, Routledge, pp.140- 145 (2004)
Y. Kawazoe & D. Suzuki

Comparison of the 40 mm ball with the 38 mm ball impacted to the table tennis racket based on the predicted impact phenomena

Y. Kawazoe* and D. Suzuki**

* *Department of Mechanical Engineering, Saitama Institute of Technology 1690, Okabe, Saitama, 369-0293, JAPAN*
** *Hitachi Kodaira Semicon Ltd., Tokyo*

1 Introduction

Previous papers (Kawazoe 1992, Kawazoe *et al.*, 2002 a, 2002 b, 2003) investigated the physical properties of the table tennis racket and the ball, and predicted the impact force, the contact time, the deformation of ball and rubber, the coefficient of restitution, the racket rebound power and the shock vibrations associated with the frontal impact when the impact velocity and the impact location on the racket face are given. It is based on the experimental identification of the dynamic characteristics of the ball-racket- arm system and an approximate nonlinear impact analysis. Also considered are the shock vibrations at the grip portion of the racket handle. The results showed that the rebound power coefficient decreases remarkably with increasing impact velocity. Although a player's arm has a remarkable effect on the reduced mass of racket, it has almost no effect on the rebound ball velocity because the mass of a ball is too small compared to the mass of a racket itself.

This study compares the new larger 40 mm ball with the 38 mm ball in terms of the impact force, the contact time, the deformation of the ball and rubber, the coefficient of restitution and the rebound power coefficient associated with the impact between the table tennis racket and the ball when the impact velocity and the impact locations on the racket face are given. It is based on the predicted results using the experimentally identified dynamic characteristics of the ball-racket system and the approximate nonlinear impact analysis (Kawazoe 2002 a, 2002 b, 2003).

2 Nonlinear restoring force characteristics of balls and rubbers

The predicted performance of table tennis racket relating to the rebound power when using a 40 mm ball (2.7 g) is compared to that when using a 38 mm ball (2.5 g). The mass of a racket (BISIDE) is 171 g including 79.5 g of the rubbers (SRIVER). Table 1 shows the physical properties of the table tennis racket used in the study.

Figure 1 shows schematically the compression test for obtaining the applied force-deformation curves, where the ball was deformed between two flat surfaces as shown in (a) and the ball plus rubbers were deformed with a racket head clamped as shown in (b). Figure 2 shows the results of the compression test of balls. Figure 3 is the results of compression test of composed ball/rubbers systems with a 40 mm and a 38 mm ball.

Assuming that a ball deforms only at the side in contact with the rubbers, the curves of restoring force vs. ball deformation, restoring force vs. rubbers deformation, and the restoring force vs. deformation of the composed ball/rubbers system are obtained from the results of applied force-deformation tests.

Figure 4 shows the deformation X_B of a ball against the applied force assuming that a ball deforms only at the side in contact with the rubber. Figure 5 shows the deformations X_R of rubbers with a 40 mm ball and a 38 mm ball against the applied force. Figure 6 shows the restoring forces vs. deformations of the composed rubber/ball systems with a 40 mm ball and a 38 mm ball. These restoring characteristics are determined in order to satisfy a number of experimental data using the

Table 1 Physical properties of table tennis racket used in the study.

Racket	BISIDE with rubber	BISIDE without rubber
Face area	185 cm^2	185 cm^2
Mass	171g	91.5g
Center of gravity from grip end	147 mm	130 mm
Moment of inertia I_{GY} about Y axis	2.51gm^2	1.10 gm^2
Moment of inertia I_{GX} about X axis	0.26 gm^2	0.16 gm^2
1st frequency	253 Hz	351 Hz

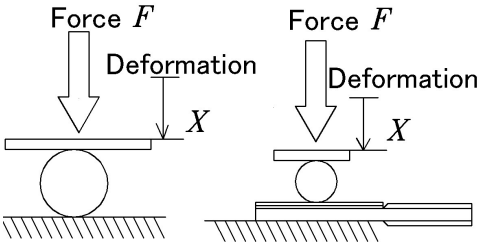

(a) Ball (b) Ball and Rubbers system
Fig.1 Illustrated applied force - deformation test

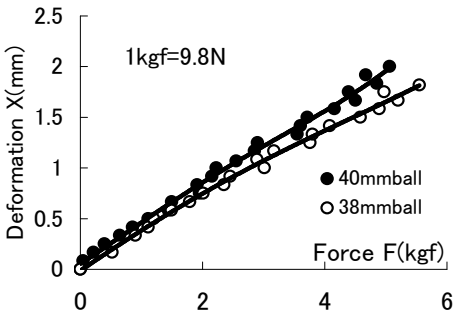

Fig.2 Rresults of the compression test of balls. (1 kgf = 9.8 N).

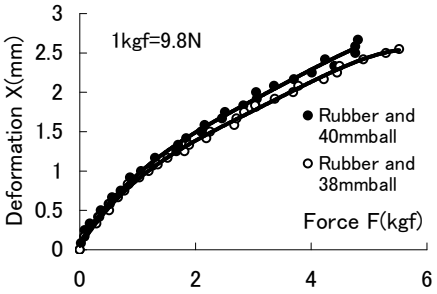

Fig.3 Results of compression test of composed rubbers & ball systems. (1 kgf = 9.8 N).

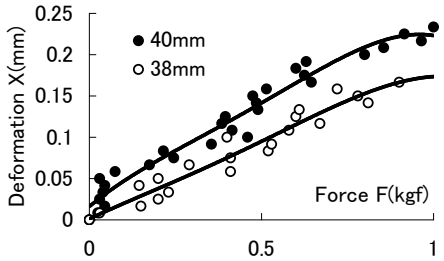

Fig.4 Deformations X_B of ball s against the applied force assuming that balls deform only at the side in contact with the rubbers. (1 kgf = 9.8 N).

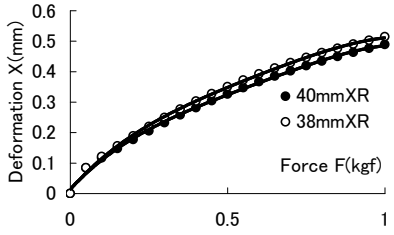

Fig.5 Deformations X_R of rubbers with a 40 mm ball and a 38 mm ball against the applied force.

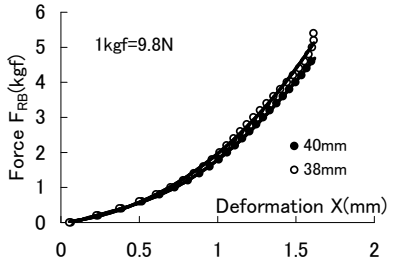

Fig.6 Restoring forces vs. deformations of the composed rubber/ball systems with a 40 mm ball and a 38 mm ball.

least squares method.

The curves of the corresponding stiffness are derived by differentiation of the equations of restoring force with respect to deformation. Figure 7 is the stiffness vs. deformations of the composed ball/rubber systems with a 40 mm ball and a 38 mm ball. The stiffnesses of composed ball/rubbers systems exhibit the non-linearity. Figure 8 is the restoring force vs. stiffness of the composed ball/rubber systems with a 40 mm ball and a 38 mm ball.

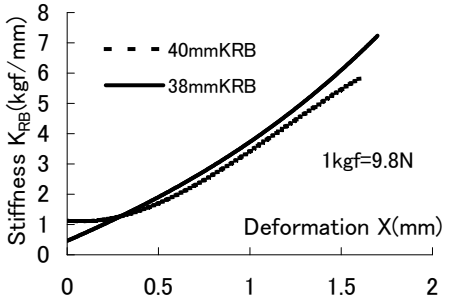

Fig.7 Comparison of stiffness vs. deformations of the composed ball/rubber systems with a 40 mm ball and a 38 mm ball.

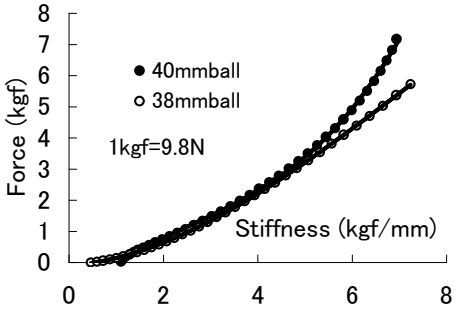

Fig.8 Comparison of restoring force vs. stiffness of the composed ball/rubber systems with a 40 mm ball and a 38 mm ball .

3 Energy losses in a collision between a ball and rubbers

Figure 9 shows the illustrated collision test between a ball and clamped rubbers for estimation of energy loss of the ball and the rubbers. Figure 10 shows the measured coefficient of restitution e_r (= $V_B/V_{B\,o}$) vs. incident velocity $V_{B\,o}$ of the 40 mm ball impacted to the clamped rubbers compared to that of the 38 mm ball. Figure 11 shows the computation of the velocities from recorded high-speed videos for the measurement of coefficient of restitution between ball and clamped rubber.

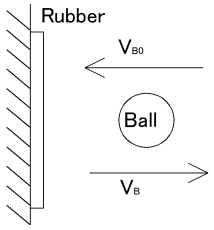

Fig.9 Illustrated collision test between a ball and clamped rubbers for estimation of energy loss of the ball and the rubbers.

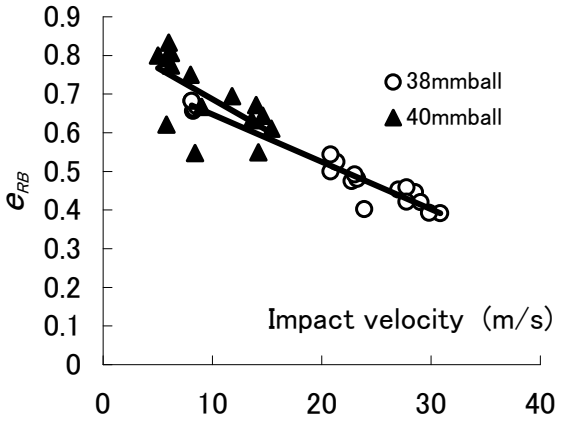

Fig.10 Measured coefficient of restitution of the 40 mm ball impacted to the clamped rubbers compared to the 38 mm ball.

4 Analytical results of factors associated with impact between a racket and a ball

According to the previous paper (Kawazoe *et al.* 2002 a, 2002 b, 2003), we can predict the contact time T_c, the impact force $F(t) = F_{max}\sin(\pi t/T_c)$, $(0 \leqq t \leqq T_c)$, $F_{mean} = 2F_{max}/\pi$, the deformation X_B of ball and X_R of rubbers, the coefficient of restitution e_r, the racket rebound power coefficient e associated with the frontal impact when the impact velocity and the impact location on the racket face are given.

Figure 12 shows the tested racket BISIDE with rubber SRIVER (1.9 mm sponge, Tamasu

(a) Pre-impact: Initial position

(c) Post-impact: Initial position

(b) Pre-impact: position after 2 ms

(d) Post-impact: position after 2 ms

Fig.11 Computation of the velocities from recorded high-speed videos for the measurement of coefficient of restitution between ball and clamped rubber.

Fig.12 Tested racket BISIDE with rubber SRIVER (1.9 mm sponge).

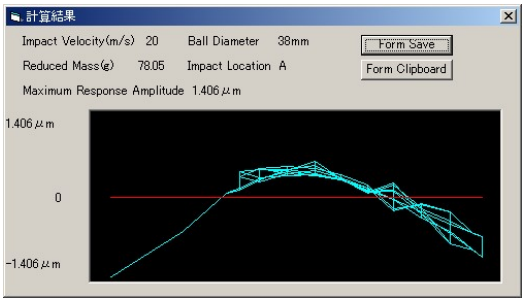

Fig.13 Predicted initial amplitude of table tennis racket vibration component when a ball hits a racket at impact location A (Top side) with a velocity of 20 m/s using performance prediction system developed in this study.

Co. Ltd., Tokyo, Japan). Figure 13 shows the predicted initial amplitude of table tennis racket vibration (1st mode component) when a ball hits a racket at impact location A (Top side) with a velocity of 20 $m \cdot s^{-1}$ using the performance prediction system developed in this study.

Figure 14 shows the predicted impact force F_{mean} vs. impact velocity when a ball strikes the center of racket face (impact location: D). Compared to the 38 mm ball, the impact force with 40 mm ball is slightly larger.

Figure 15 shows the predicted contact time T_c vs. impact velocity when a ball strikes the centre of racket face. The contact time with 40 mm ball is shorter below 15 m/s and longer above 15 $m \cdot s^{-1}$ of impact velocity. The reason that the contact time is shorter below 15 m/s and longer above 15 $m \cdot s^{-1}$ of impact velocity and the rebound power coefficient is slightly larger below 20 $m \cdot s^{-1}$ but smaller above 20 $m \cdot s^{-1}$ of impact velocity with the 40 mm ball than those with 38 mm ball is due to the experimental fact that the stiffness of the composed rubber/ball system is larger, the energy loss of the ball and the rubber during impact is also larger and the deformation of rubbers are larger at the lower impact velocities and smaller at the higher impact velocities with the 40 mm ball than those with 38 mm ball.

Figure 16 shows the predicted deformation of the ball vs. impact velocity when a ball strikes the center of racket face. The deformation of the ball with 40 mm ball is much larger than that with

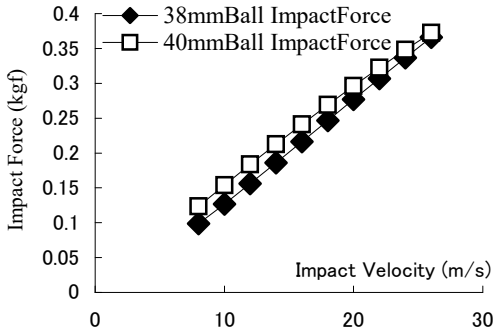

Fig.14 Predicted impact force vs. impact velocity when a ball strikes the center of racket face. The impact force with 40 mm ball is slightly larger than that with 38 mm ball (1kgf= 9.8 N).

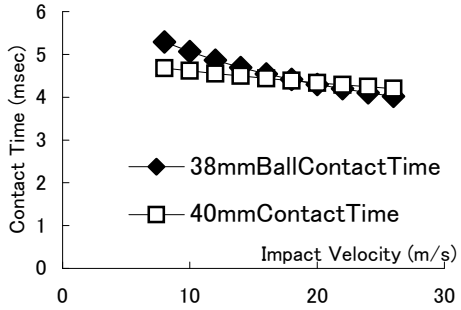

Fig.15 Predicted contact time vs. impact velocity when a ball strikes the center of racket face. The contact time with 40 mm ball is shorter below 15 $m \cdot s^{-1}$ and longer above 15 $m \cdot s^{-1}$ of impact velocity than that with 38 mm ball.

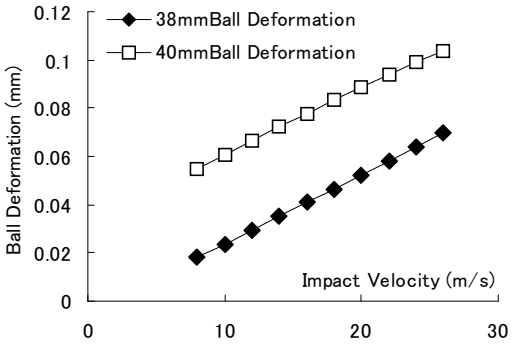

Fig.16 Predicted deformation of the ball vs. impact velocity when a ball strikes the center of racket face. The deformation of the ball with 40 mm ball is much larger.

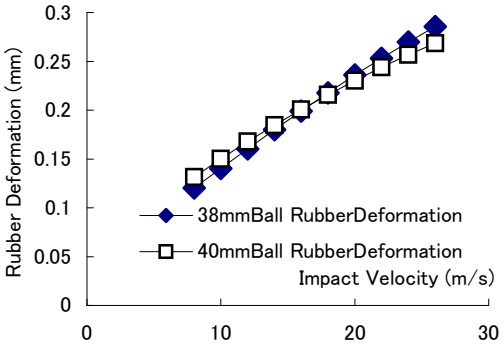

Fig.17 Predicted deformation of the rubber vs. impact velocity when a ball strikes the center of racket face. The deformations of the rubbers are almost the same.

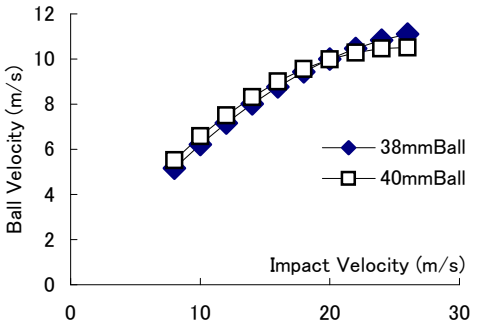

Fig.18 Predicted rebound ball velocity vs. impact velocity when a ball strikes the center on the racket face.

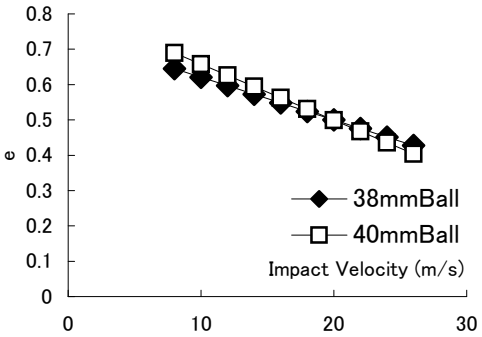

Fig.19 Predicted rebound power coefficient e when a ball strikes the center on the racket face at the velocity of 30 $m \cdot s^{-1}$. The rebound power coefficient with 40 mm ball is slightly larger below 20 $m \cdot s^{-1}$ but smaller above 20 $m \cdot s^{-1}$ of impact velocity.

38 mm ball. Figure 17 shows the predicted deformation of the rubber vs. impact. The deformations of the rubbers are almost the same.

Figure 18 is the predicted rebound ball velocity vs. impact velocity when a ball strikes the center on the racket face. Figure 19 is the predicted rebound power coefficient *e* when a ball strikes the center on the racket face at the velocity of 30 m/s. The rebound power coefficient *e* with 40 mm ball is slightly larger below 20 m/s but smaller above 20 m/s of impact velocity.

5 Conclusions

The predicted racket performances regarding the rebound power of a 40 mm ball (2.7 g) were compared to those of a 38 mm ball (2.5 g) using a racket with mass of 171 g including 79.5 g of rubbers. With the 40 mm ball compared to the 38 mm ball, the impact force is slightly larger, the contact time is shorter below 15 $m \cdot s^{-1}$ and longer above 15 $m \cdot s^{-1}$ of impact velocity, the deformation of the ball is much larger but that of the rubber is almost the same, and the rebound power coefficient is slightly larger below 20 $m \cdot s^{-1}$ but smaller above 20 $m \cdot s^{-1}$ of impact velocity. Accordingly the post-impact velocity of the 40 mm ball is slightly faster below 20 $m \cdot s^{-1}$ of impact velocity and slower above 20 $m \cdot s^{-1}$ compared with those of the 38 mm ball. Since the drag force of 40 mm ball is larger than that of 38 mm ball, the velocity of 40 mm ball should be slower.

The reason that the contact time is shorter below 15 $m \cdot s^{-1}$ and longer above 15 $m \cdot s^{-1}$ of impact velocity and the rebound power coefficient is slightly larger below 20 $m \cdot s^{-1}$ but smaller above 20 $m \cdot s^{-1}$ of impact velocity with the 40 mm ball than those with 38 mm ball is due to the experimental fact that the stiffness of the composed ball/rubber systems is larger, the energy loss of the ball and the rubber during impact is also larger and the deformation of rubbers are larger at the lower impact velocities and smaller at the higher impact velocities with the 40 mm ball than those with 38 mm ball.

Acknowledgments

The authors are grateful to Prof. Masuda of Saitama Institute of Technology for his help in the compression test of ball and rubber, and also to the research members at Tamasu Co. Ltd. (Tokyo, Japan) for their help in a part of the impact test. This study was also supported by the High-Tech Research Center of Saitama Institute of Technology.

References

Kawazoe,Y. (1992), Ball/Racket Impact and Computer Aided Design of Rackets. **International Journal of Table Tennis Sciences**, 1, 9-18.

Kawazoe,Y. and Suzuki, D. (2002 a) Mechanism of Restitution Coefficient and Impact Factors between a Ball and a Racket in Table Tennis. **The Book of the 4th International Conference on the Engineering of Sport** (edited by the Japanese Sports Engineering Association and Japan Society of Mechanical Engineers), pp.58-63.

Kawazoe,Y. and Suzuki, D. (2002 b) Prediction of Rebound Velocity of the 40 mm New Ball Compared to the 38 mm Ball Impacted to the Table Tennis Racket. **The Book of the 4th International Conference on the Engineering of Sport** (edited by the Japanese Sports Engineering Association and Japan Society of Mechanical Engineers), pp.64-69.

Kawazoe, Y. and Suzuki, D. (2003) Impact prediction between a ball and racket in terms of contact forces, contact times, restitution coefficients and sweet spot in table tennis. **Science and Racket Sports 3** (edited by), in press